Published in final edited form as:
Curr Biol. 2011 September 27; 21(18): 1578–1583. doi:10.1016/j.cub.2011.08.021.

Organization of the Smallest Eukaryotic Spindle

Lu Gan[1], **Mark S. Ladinsky**[1], and **Grant J. Jensen**[1,2]

[1]Division of Biology, California Institute of Technology, Pasadena, CA, 91125, USA

[2]Howard Hughes Medical Institute, California Institute of Technology, Pasadena, CA, 91125, USA

Summary

Studies of mitosis in metazoans, plants, and fungi have converged on a highly conserved model of mitosis in which paired sister chromatids attach to kinetochore microtubules (kMTs) emanating from opposite spindle poles. Once each chromosome is attached to one or more of its own kMTs, the spindle checkpoint is released, the anaphase-promoting complex is activated and sister-chromatid cohesion is lost. Different species vary, however, in both the ultrastructure and timing of these events [1–4]. Some unicellular eukaryotes, for instance, have been reported to have fewer kMTs than chromosomes [4, 5]. If true, this would be important because it is unclear how the spindle checkpoint could be satisfied. In the vast majority of these studies, however, mitotic cells were chemically fixed at room temperature and then stained. Because chemical fixation is slow (taking from seconds to hours), dynamic and/or small structures like spindle MTs and kinetochores are not always preserved, leaving substantial uncertainty [6]. Indeed in some of these cases, later higher-resolution studies have reversed earlier claims [7–11]. Here we show that in *Ostreococcus tauri* (the smallest eukaryote known), mitosis does indeed involve fewer spindle microtubules than chromosomes. *O. tauri* cultures were artificially arrested in mitosis and then using electron tomography of high-pressure-frozen cells, spindles were imaged both in plastic and in a near-native ("frozen-hydrated") state in 3-D to "macromolecular" resolution. Mitotic cells have a distinctive heterochromatin-free “spindle tunnel” in their nuclei with ~4 short, incomplete (unclosed) microtubules at each end of the spindle tunnel. In addition, up to two long microtubules extend into the center of the spindle tunnel. *O. tauri*'s spindle checkpoint machinery seems typical, however, since inhibitors of microtubule polymerization and proteasomes stall mitosis, and homologs of many known spindle checkpoint genes are present in the genome. Taken together, these data suggest that *O. tauri*'s 20 chromosomes are physically bundled and segregated as just one or a small number of groups.

Results and Discussion

Detection and enrichment of mitotic cells

The *O. tauri* cell cycle can be loosely synchronized with light, resulting in early interphase cells at the dark-to-light transition (morning) and mitotic cells at the light-to-dark transition (evening) [12]. In our previous electron cryotomography study of evening cells, however, no

Correspondence should be addressed to G.J.J. (jensen@caltech.edu). Phone: (626) 395 8827, Fax: (626) 395 5730.

Supplemental Information
Supplemental Information includes Experimental Procedures, four figures, three tables, one movie, and Supplemental Text and can be found with this article online at doi:XYZ.

spindles were detected [13]. At the time, we did not have a method to determine the percentage of mitotic cells, so we did not know if mitotic cells were completely absent in those naturally synchronized samples or if mitosis was simply so fast that none happened to be seen in our limited pool. We therefore developed an immunofluorescence assay to detect phospho-histone H3 [14], which is found in mitotic (H3P+) but not interphase cells (H3P-) (Supplemental Text and Figures S1 A–C).

Using the H3P assay, we modified an artificial synchronization protocol that involved sequential drug treatments and washouts to arrest cells at successive stages of the cell cycle [15] (Table S1A, Supplemental Text). Briefly, cells were first arrested at the G1/S transition with hydroxyurea, a DNA-synthesis inhibitor. Following a 9-hour incubation, the hydroxyurea was washed out and then propyzamide, a tubulin-polymerization inhibitor, was added [16]. This allowed the cells to progress to prophase. Finally, following a 12-hour incubation, the propyzamide was washed out and replaced with proteasome inhibitor MG132 [17]. This allowed the MTs to recover, but arrested the cells in metaphase (39% mitotic cells, see Figure S1). Control experiments showed that the drug treatments were reversible and only slightly perturbed cell-culture viability (Figure S2). Together, these results indicate not only that *O. tauri* mitosis requires functional spindle MTs, but also that the majority of propyzamide-arrested cells pass through mitosis within an hour after the drug's removal. Thus, the spindles in the "MG132-treated" cells imaged throughout the study must be functional.

Mitotic nuclei have substantially fewer than 40 microtubules

MG132-treated cells were first imaged intact, plunge-frozen (Figure S3A and S3B). Many of these cells were two or more times thicker than the mean-free path of the electrons, however, reducing the quality of the tomographic reconstructions and restricting analysis to the smaller cells. None of these smaller cells exhibited a mitotic spindle.

To obtain images of the thicker, likely-mitotic cells, cell pellets were high-pressure-frozen, freeze-substituted, plastic-embedded, and sectioned. Tomograms of single plastic sections showed that MG132-treated cells were ovoid (1.5 – 2 μm long and ~ 1 μm wide), with the nucleus in the middle and chloroplasts at the cell poles (Figure S3C and S3D). Nuclei were ~ 0.7 μm wide. In the middle of mitotic nuclei there was a heterochromatin-free zone that we refer to as the "spindle tunnel," which contained spindle MTs. The spindle tunnel flared out at its ends to 218 ± 16 nm (n = 16) and narrowed to only ~100 nm near its midpoint. Longitudinal sections (parallel to tunnel) showed that most spindle tunnels (7 of 10) contained one or two long, incomplete MTs (Figures S4 A–C). Transverse sections (perpendicular to tunnel) through the ends of spindle tunnels consistently showed 4 ± 2 short MTs (n = 9), which often had “C”-shaped cross-sections (Figure S4 D–F). No nuclear envelope was seen at the poles (the ends of the spindle tunnel where the spindle MTs terminated), suggesting that mitosis is semi-open. Centrosomes and spindle pole bodies were also not seen and no astral MTs were detected in the cytoplasm outside the nucleus.

To obtain more complete views, the nuclei of four cells were reconstructed in their entirety by merging dual-axis tomograms from 3–4 serial 200-nm sections [18]. All four mitotic nuclei exhibited hourglass-shaped tunnels (Figure 1, Movie S1). Three of the four serially-sectioned cells were sectioned nearly transverse to the tunnel (Figure 1A–C) and contained several short spindle MTs at the poles. These short MTs (<100 nm) were roughly parallel and clustered together, with nearest-neighbor distances of 40–50 nm. Additionally, incomplete long MTs penetrated into the middle of three of the tunnels (Figures 1A, 1), in some cases almost reaching the opposite pole (Figure 1D), likely serving as polar MTs analogous to the long MTs in other eukaryotes. Negative-control tomograms of interphase

cells confirmed that spindle tunnels are only found in mitotic cells (Figure S4 G–H, Supplemental Text).

O. tauri spindle MTs are rarely complete tubes

To obtain higher-resolution images of the spindles in a closer-to-native state, we cryosectioned high-pressure-frozen MG132-treated cells and imaged them in the frozen-hydrated state. Cells were selected at random because neither the spindle tunnel nor spindle MTs could be seen in the low-dose low-magnification images used to locate cells for cryotomography. Each cryosection (nominally ~150-nm thick) contained only ~1/4th to 1/5th of the typically ~700-nm-wide nucleus, meaning that only a random portion of a spindle could be imaged in each tomogram. Cryosections taken transverse to the spindle axis and near the pole were the most informative because they provide the most accurate estimate of MTs in a half spindle. Several hundred (356) cryosections were imaged and analyzed to ensure no structures were missed (Table S1). Portions of spindles were found in 44 cryosections, organized into small clusters of parallel MTs (Figure 2). None of the clusters had more than 5 MTs, confirming the low numbers seen in the plastic sections.

The resolution of the cryosection tomograms was sufficient to discern individual protofilaments (Figures 2 and 3 and Table S2). While occasionally one or two long (>200 nm) MTs were seen, the majority of the spindle MTs were shorter than 100 nm (15 of 24 not truncated by the cryosectioning), corresponding to less than twelve (8-nm long) α-β tubulin dimers. Some MTs were only ~50 nm long (Figure 3: MTs 10, 19, and 20), corresponding to just a few α-β tubulin dimers. When the end structures were clear, MTs were seen to have one conical and one open end (Figure 3: MTs 10, 19, and 26) or two open ends (MTs 14 and 20). While the conical caps were likely the cone-shaped γ-tubulin complex [19], the MTs with two open ends may have been nucleated by some γ-tubulin-independent mechanism as has been observed in other organisms [20, 21]. Since neither spindle-pole bodies nor centrosomes were seen, as has been the case in various plant cells [22], it remains to be determined how *O. tauri* spindle MTs organize at the poles.

Most of the MTs had fewer than 13 protofilaments (4 to 12), and had C-shaped cross-sections. MTs with C-shaped cross-sections have been found in the spindles of other organisms [23–25], but the short C-shaped region (0.1–0.5 μm long) was located at the plus ends of MTs, often near the middle of the spindles. MTs with the fewest protofilaments – as few as four (MT 5 in Figure 3) –had flatter cross-sections. Side views of these MTs often showed a slight curve along the protofilament axis. We did not observe MT protofilaments in the highly curved “rams horn” motif that has been reported for MTs shrinking *in vitro* [26, 27]. While the structure of *O. tauri* MTs were reminiscent of the nearly flat sheets seen at the plus ends of MTs growing *in vitro* [26, 27], recent electron tomography studies showed that MTs growing *in vivo* had flared plus-end morphologies instead [28, 29]. Therefore, while the MTs were likely undergoing rapid dynamics, we cannot conclude whether the *O. tauri* spindle MTs were growing or shrinking based on their morphology.

The spindle microtubules seen were likely functional mitotic structures

Control experiments confirmed that spindle MTs were exclusive to mitotic (H3P+) cells (Supplemental Text). To check whether the MG132 treatment was influencing the appearance of the spindle MTs, causing them to appear incomplete, we analyzed the structures of cytoplasmic MTs in the same cells. Cytoplasmic MTs in the MG132-treated cells appeared complete in tomographic slices perpendicular to the MT axis and had the 25-nm-wide double-line motif in tomographic slices parallel to the MT axis (Figure 3), just like the cytoplasmic MTs seen in plunge-frozen interphase *O. tauri* cells [13] and cells long after the propyzamide was washed out. This proves that the tubulin in these cells was able to form

complete MTs. Cryotomograms of cells that were high-pressure-frozen between 10 and 20 minutes after the propyzamide washout and without any MG132 treatment at all also showed the same characteristics of low number (~4), short length (<100 nm), and frequent lack of complete walls. Many of these were in the midst of mitosis, since immunofluorescence images showed that 50% (n = 252) of the cells were H3P+ before the high-pressure-freezing step and only 26% (n = 261) of the cells were H3P+ after. MG132 therefore did not appear to influence the structure of spindle MTs.

O. tauri has less than one MT per chromosome

While it has been claimed in the past that certain unicellular eukaryotes undergo mitosis with fewer MTs than chromosomes, uncertainties in the numbers of chromosomes and limitations of traditional EM techniques to preserve short MTs and small kinetochores has left considerable room for doubt (Supplemental Text). Using tomography of rapidly frozen cells, including cryosectioned cells preserved in a near-native, "frozen-hydrated" state, here we observed that mitotic *O. tauri* cells exhibited far fewer spindle MTs (~10) than chromosomes (40). The spindle MTs were arranged as a small cluster of approximately four, short, incomplete MTs at each spindle pole and one or two long MTs extending into a spindle tunnel (Figure 4). Further, since (1) the spindle poles were so small (~200 nm diameter), (2) the center-to-center MT spacing varied between 40–50 nm, and (3) there was no apparent ordered packing, there simply was not enough room for many more MTs. Because the difference between the number of chromosomes and spindle MTs counted is so great, and the total number of partial and full spindles imaged was so large (13 partial and 4 full spindles in plastic sections and 64 partial spindles in cryosections), it is very unlikely that our survey would have missed a full (21-MT) half-spindle, had it existed. We conclude that *O. tauri* segregates its chromosomes with less than one MT per chromosome.

Possible mechanisms for *O. tauri* chromosome segregation

Another class of photosynthetic plankton, the diatoms, reportedly use an actin/myosin-based spindle "matrix" to move the chromosomes to the spindle poles and keep them there until the end of mitosis [30] (Supplemental Text). While actin-like filaments are routinely visible in cryotomograms of small cells [31, 32], no such matrix was seen here in *O. tauri*. *O. tauri* mitosis was also clearly MT-dependent, since it was arrested by propyzamide, a tubulin-polymerization inhibitor.

Kinetochores were also not identified in the tomograms, but two lines of evidence suggest that *O. tauri* chromosomes have them. First, all known MT-related mitotic arrests are caused by the spindle checkpoint, which is generated by kinetochores [33]. Because *O. tauri* mitosis was arrested by propyzamide, it likely has a spindle checkpoint. Second, homologs of many kinetochore genes are present in the *O. tauri* genome, including Nuf2, Ndc80, CENP-C, Bub3, Mad2, Mad3, Cdc20, Aurora B, Bub1, Mad1, Polo kinases, and a CenH3 candidate [34]. We have now shown that *O. tauri* at least has a functional Aurora B kinase because the mitotic cells have the H3P epitope, which is generated by Aurora B in other eukaryotes [35]. *O. tauri*'s kinetochores were probably too small to be recognized, perhaps like the tiny *S. cerevisiae* “point” kinetochores [36] which have also not yet been seen by EM [37].

How then does *O. tauri* segregate its 20 chromosome pairs with so few kMTs? At least two possibilities should be considered. First, individual kMTs or the entire kMT bundle might attach to a single chromosome, and move chromosomes one or a few at a time. Such a mechanism would require major adaptations, however, like tethering segregated chromosomes to the spindle pole and then resetting the spindle checkpoint. We are not aware of any precedent for this, and judge the required complexities unlikely. In the second model, if the twenty *nonhomologous* chromosomes were physically linked at metaphase,

they could be segregated together by a smaller number of kMTs. The spindle checkpoint could be satisfied if each chromosome (with its own checkpoint-signaling complex) attached to a common kinetochore, possibly akin to kinetochore clustering in *S. pombe* and maize [38, 39] (Supplemental Text). This model might also explain chromosome segregation in *Trypanosoma brucei* (~27 larger chromosomes and ~8 kinetochores, see Supplemental Text) and other picoplankton [40, 41].

Supplementary Material

Refer to Web version on PubMed Central for supplementary material.

Acknowledgments

We thank Drs. G. Henderson, P. Dias, A. McDowall, F-Y Bouget, H. Moreau, W. Marshall, J. Azimzadeh, and G. Ou for discussions, and the Reviewers for helpful comments. This work was supported in part by NIH grant P50 GM082545 to GJJ and a gift to Caltech from the Gordon and Betty Moore Foundation. LG is a Damon Runyon Fellow supported by a fellowship from the Damon Runyon Cancer Research Foundation (DRG-1940-07). MSL was supported by NIH grant 2 R37 AI041239-06A1 to P. Björkman.

References

1. Grell, K. Protozoology: with 15 tab. Berlin, Heidelberg, New York: Springer; 1973.
2. Kubai DF. The evolution of the mitotic spindle. Int Rev Cytol. 1975; 43:167–227. [PubMed: 816751]
3. Heath IB. Variant mitoses in lower eukaryotes: indicators of the evolution of mitosis. Int Rev Cytol. 1980; 64:1–80. [PubMed: 20815116]
4. Raikov, IB. The protozoan nucleus, morphology and evolution. Wien; New York: Springer-Verlag; 1982.
5. Daniels JP, Gull K, Wickstead B. Cell biology of the trypanosome genome. Microbiol Mol Biol Rev. 2010; 74:552–569. [PubMed: 21119017]
6. McDonald KL, Auer M. High-pressure freezing, cellular tomography, and structural cell biology. BioTechniques. 2006; 41:137, 139, 141. passim. [PubMed: 16925014]
7. Franke WW, Reau P. The mitotic apparatus of a zygomycete, Phycomyces blakesleeanus. Arch Mikrobiol. 1973; 90:121–129. [PubMed: 4350549]
8. McCully EK, Robinow CF. Mitosis in Mucor hiemalis. A comparative light and electron microscopical study. Arch Mikrobiol. 1973; 94:133–148. [PubMed: 4778923]
9. Heath IB, Rethoret K. Mitosis in the fungus Zygorhynchus moelleri: evidence for stage specific enhancement of microtubule preservation by freeze substitution. Eur J Cell Biol. 1982; 28:180–189. [PubMed: 7173217]
10. McCully EK, Robinow CF. Mitosis in the fission yeast Schizosaccharomyces pombe: a comparative study with light and electron microscopy. Journal of Cell Science. 1971; 9:475–507. [PubMed: 4108061]
11. Ding R, McDonald KL, McIntosh JR. Three-dimensional reconstruction and analysis of mitotic spindles from the yeast, Schizosaccharomyces pombe. J Cell Biol. 1993; 120:141–151. [PubMed: 8416984]
12. Farinas B, Mary C, de O Manes CL, Bhaud Y, Peaucellier G, Moreau H. Natural synchronisation for the study of cell division in the green unicellular alga Ostreococcus tauri. Plant Mol Biol. 2006; 60:277–292. [PubMed: 16429264]
13. Henderson G, Gan L, Jensen G. 3-D ultrastructure of O. tauri: electron cryotomography of an entire eukaryotic cell. PLoS ONE. 2007; 2:e749. [PubMed: 17710148]
14. Hendzel MJ, Wei Y, Mancini MA, Van Hooser A, Ranalli T, Brinkley BR, Bazett-Jones DP, Allis CD. Mitosis-specific phosphorylation of histone H3 initiates primarily within pericentromeric heterochromatin during G2 and spreads in an ordered fashion coincident with mitotic chromosome condensation. Chromosoma. 1997; 106:348–360. [PubMed: 9362543]

15. Corellou F, Camasses A, Ligat L, Peaucellier G, Bouget FY. Atypical regulation of a green lineage-specific B-type cyclin-dependent kinase. Plant Physiology. 2005; 138:1627–1636. [PubMed: 15965018]
16. Akashi T, Izumi K, Nagano E, Enomoto M, Mizuno K, Shibaoka H. Effects of Propyzamide on Tobacco Cell Microtubules In vivo and In vitro. Plant and Cell Physiology. 1988; 29:1053–1062.
17. Genschik P, Criqui MC, Parmentier Y, Derevier A, Fleck J. Cell cycle-dependent proteolysis in plants. Identification Of the destruction box pathway and metaphase arrest produced by the proteasome inhibitor mg132. Plant Cell. 1998; 10:2063–2076. [PubMed: 9836745]
18. Ladinsky MS, Mastronarde DN, McIntosh JR, Howell KE, Staehelin LA. Golgi structure in three dimensions: functional insights from the normal rat kidney cell. J Cell Biol. 1999; 144:1135–1149. [PubMed: 10087259]
19. Moritz M, Braunfeld MB, Guenebaut V, Heuser J, Agard DA. Structure of the gamma-tubulin ring complex: a template for microtubule nucleation. Nature cell biology. 2000; 2:365–370.
20. Mahoney NM, Goshima G, Douglass AD, Vale RD. Making microtubules and mitotic spindles in cells without functional centrosomes. Current biology : CB. 2006; 16:564–569. [PubMed: 16546079]
21. Kitamura E, Tanaka K, Komoto S, Kitamura Y, Antony C, Tanaka TU. Kinetochores generate microtubules with distal plus ends: their roles and limited lifetime in mitosis. Developmental Cell. 2010; 18:248–259. [PubMed: 20159595]
22. Wasteneys GO. Microtubule organization in the green kingdom: chaos or self-order? Journal of Cell Science. 2002; 115:1345–1354. [PubMed: 11896182]
23. Cohen WD, Gottlieb T. C-microtubules in isolated mitotic spindles. J Cell Sci. 1971; 9:603–619. [PubMed: 5169780]
24. Jensen C, Bajer A. Spindle Dynamics and Arrangement of Microtubules. Chromosoma. 1973; 44:73–89.
25. McIntosh JR, Roos UP, Neighbors B, McDonald KL. Architecture of the microtubule component of mitotic spindles from Dictyostelium discoideum. J Cell Sci. 1985; 75:93–129. [PubMed: 4044684]
26. Mandelkow EM, Mandelkow E, Milligan RA. Microtubule dynamics and microtubule caps: a time-resolved cryo-electron microscopy study. J Cell Biol. 1991; 114:977–991. [PubMed: 1874792]
27. Chretien D, Fuller SD, Karsenti E. Structure of growing microtubule ends: two-dimensional sheets close into tubes at variable rates. J Cell Biol. 1995; 129:1311–1328. [PubMed: 7775577]
28. Hoog JL, Huisman SM, Sebo-Lemke Z, Sandblad L, McIntosh JR, Antony C, Brunner D. Electron tomography reveals a flared morphology on growing microtubule ends. Journal of Cell Science. 2011; 124:693–698. [PubMed: 21303925]
29. Kukulski W, Schorb M, Welsch S, Picco A, Kaksonen M, Briggs JA. Correlated fluorescence and 3D electron microscopy with high sensitivity and spatial precision. The Journal of Cell Biology. 2011; 192:111–119. [PubMed: 21200030]
30. Falciatore A, Bowler C. Revealing the molecular secrets of marine diatoms. Annual review of plant biology. 2002; 53:109–130.
31. Komeili A, Li Z, Newman DK, Jensen GJ. Magnetosomes are cell membrane invaginations organized by the actin-like protein MamK. Science. 2006; 311:242–245. [PubMed: 16373532]
32. Swulius MT, Chen S, Jane Ding H, Li Z, Briegel A, Pilhofer M, Tocheva EI, Lybarger SR, Johnson TL, Sandkvist M, et al. Long helical filaments are not seen encircling cells in electron cryotomograms of rod-shaped bacteria. Biochem Biophys Res Commun. 2011; 407:650–655. [PubMed: 21419100]
33. Rieder CL, Maiato H. Stuck in division or passing through: what happens when cells cannot satisfy the spindle assembly checkpoint. Developmental Cell. 2004; 7:637–651. [PubMed: 15525526]
34. Derelle E, Ferraz C, Rombauts S, Rouzé P, Worden AZ, Robbens S, Partensky F, Degroeve S, Echeynié S, Cooke R, et al. Genome analysis of the smallest free-living eukaryote Ostreococcus tauri unveils many unique features. Proc Natl Acad Sci USA. 2006; 103:11647–11652. [PubMed: 16868079]

35. Prigent C, Dimitrov S. Phosphorylation of serine 10 in histone H3, what for? J Cell Sci. 2003; 116:3677–3685. [PubMed: 12917355]

36. Joglekar AP, Bouck DC, Molk JN, Bloom KS, Salmon ED. Molecular architecture of a kinetochore-microtubule attachment site. Nat Cell Biol. 2006; 8:581–585. [PubMed: 16715078]

37. Winey M, Mamay CL, O'Toole ET, Mastronarde DN, Giddings TH Jr, McDonald KL, McIntosh JR. Three-dimensional ultrastructural analysis of the Saccharomyces cerevisiae mitotic spindle. J Cell Biol. 1995; 129:1601–1615. [PubMed: 7790357]

38. Appelgren H, Kniola B, Ekwall K. Distinct centromere domain structures with separate functions demonstrated in live fission yeast cells. J Cell Sci. 2003; 116:4035–4042. [PubMed: 12928332]

39. Li X, Dawe RK. Fused sister kinetochores initiate the reductional division in meiosis I. Nat Cell Biol. 2009; 11:1103–1108. [PubMed: 19684578]

40. Matsuzaki M, Misumi O, Shin-I T, Maruyama S, Takahara M, Miyagishima S, Mori T, Nishida K, Yagisawa F, Nishida K, et al. Genome sequence of the ultrasmall unicellular red alga Cyanidioschyzon merolae 10D. Nature. 2004; 428:653–657. [PubMed: 15071595]

41. Worden AZ, Lee JH, Mock T, Rouzé P, Simmons MP, Aerts AL, Allen AE, Cuvelier ML, Derelle E, Everett MV, et al. Green evolution and dynamic adaptations revealed by genomes of the marine picoeukaryotes Micromonas. Science. 2009; 324:268–272. [PubMed: 19359590]

Highlights

- Cryotomography was performed on mitotic spindles in a "frozen-hydrated" state with macromolecular resolution.
- Mitotic *O. tauri* cells have 20 pairs of chromosomes but only ~10 spindle microtubules.
- Spindle microtubules range from 550 to less than 50 nm long and are mostly incomplete.
- *O. tauri* might cluster its chromosomes together at their kinetochores so they can be segregated in groups.

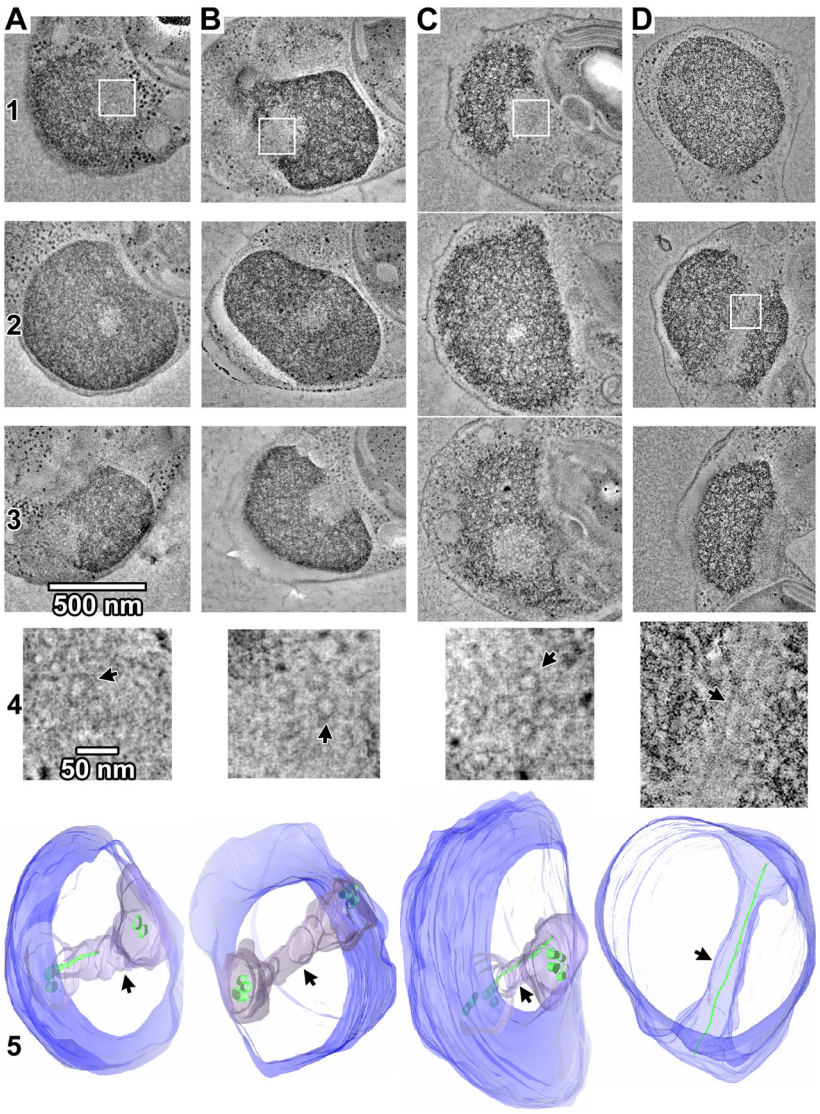

Figure 1. *O. tauri* has only a few spindle microtubules

(A–D) Tomographic slices (19 nm thick) through merged serial-section tomograms of MG132-treated, high-pressure frozen, freeze-substituted *O. tauri* cells. The entire nuclei and spindles are reconstructed in the merged tomogram. The cells in columns A-C were sectioned nearly transverse to the spindle tunnel, while the cell in column D nearly longitudinal. Rows 1 –3 show tomographic slices through upper, middle, and lower plastic sections of the nucleus. Row 4 shows enlargements of the areas boxed in white in Rows 1 or 2, with small rotations out of plane to enhance the visibility of the spindle MTs. Arrows in row 4 indicate example MTs. Row 5 shows 3-D segmentations of the chromatin boundary (blue), spindle tunnel (arrowheads), and MTs (green). Note that the tunnel-spanning portion of long MTs have incomplete walls and are modeled as thin rods instead of tubes. The cell in (B) is shown in greater detail in Movie S1.

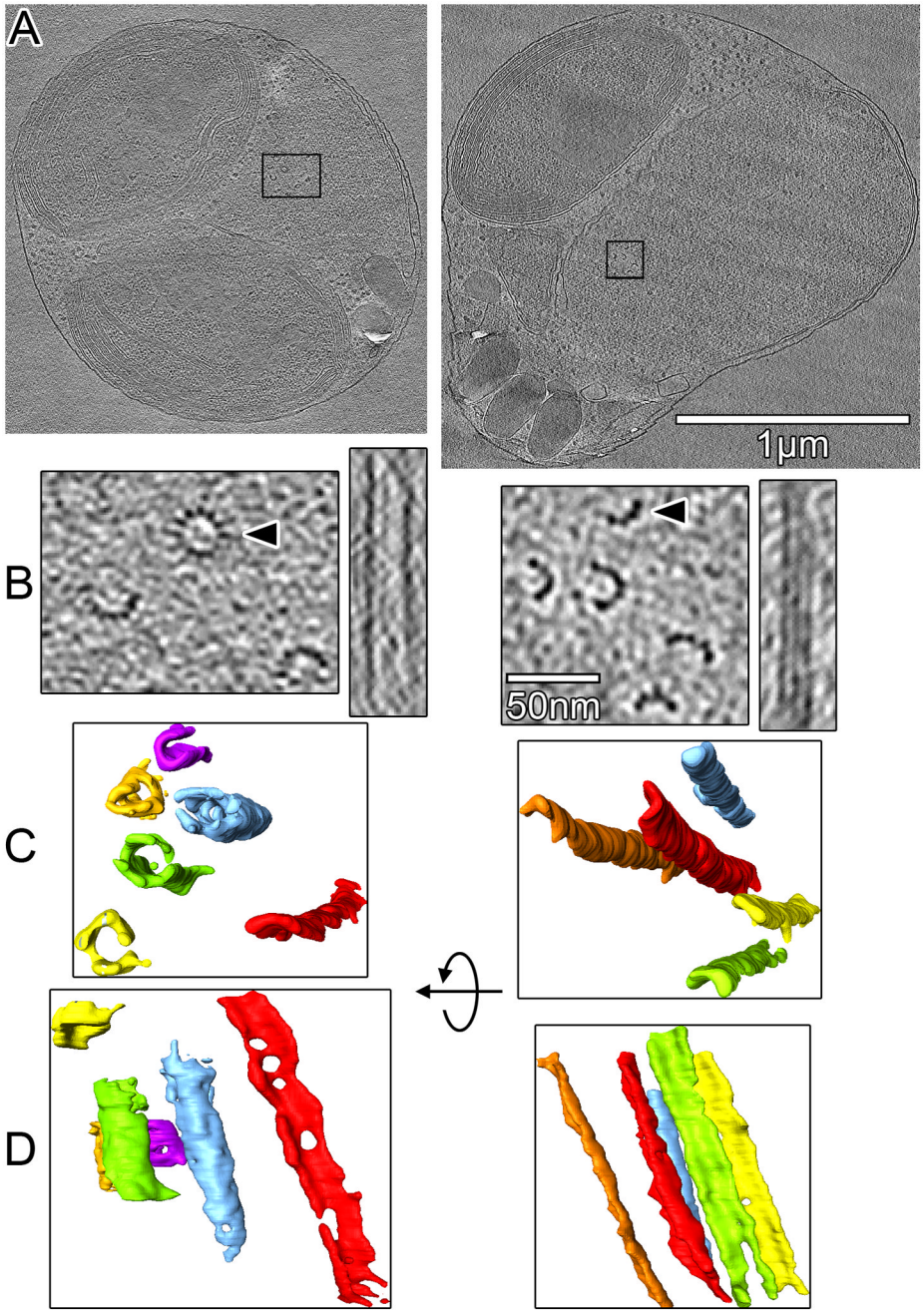

Figure 2. *O. tauri* spindle microtubules are short and mostly incomplete

(A) Tomographic slices (20 nm thick) through cryotomograms of vitreously sectioned MG132-treated cells. (B) Enlarged view of the spindle MT clusters boxed in (A). The right subpanel shows an longitudinal slice of the MT indicated by the arrowhead, taken through the center of the MT barrel (left cell) or along three protofilaments (right cell). (C, D) Segmentations of the spindle MTs in (B), colored randomly for clarity. The apparent "holes" in the MT walls are likely artifacts of the low signal-to-noise.

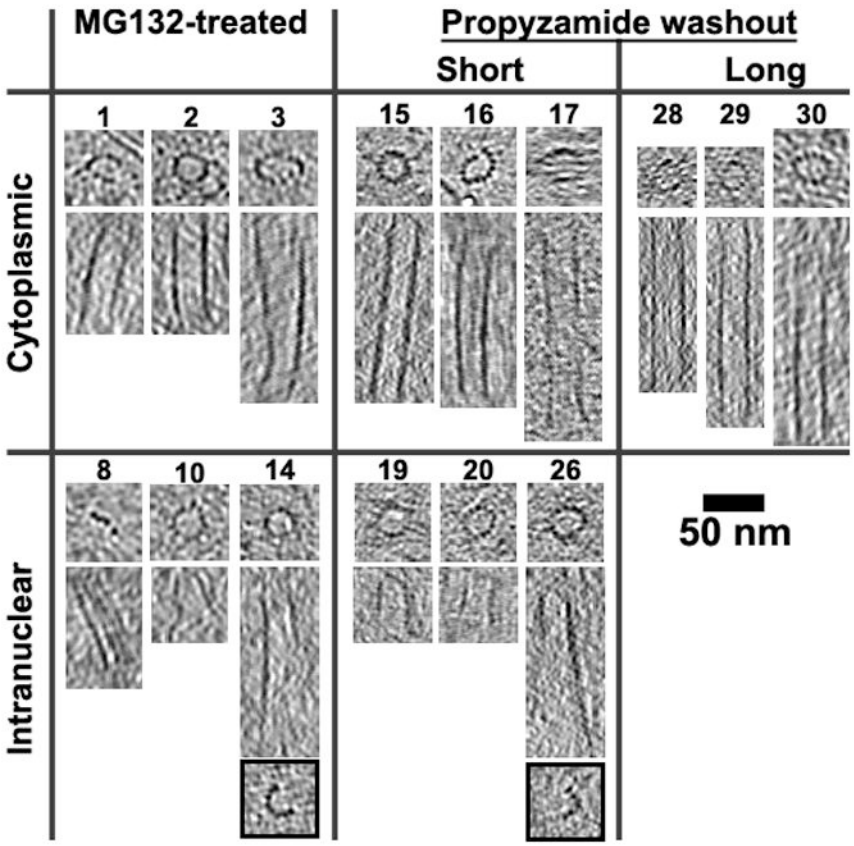

Figure 3. Example microtubules from cryosectioned cells

Tomographic slices (10 or 20 nm thick) through many MTs taken perpendicular (upper subpanels) and parallel (lower subpanels) to the MT axis. MTs 14 and 26 are complete with 13-protofilaments at one end (top subpanel) but not the other (lower subpanels with black border). In contrast to cytoplasmic MTs, which have long complete walls, most of the intranuclear (spindle) MTs are short and C-shaped along most of their length. MTs 10, 19, and 26 had one conical and one open end; MTs 14 and 20 have two open ends. Some MTs were only ~50 nm long (MTs 10, 19, and 20), which would consist of just a few α-β tubulin dimers (8-nm long). *O. tauri* spindle MTs are in general short with C-shaped profiles along most of their length, which is in agreement with the short MTs observed in the plastic-sectioned cells. See Table S2 for additional example MTs.

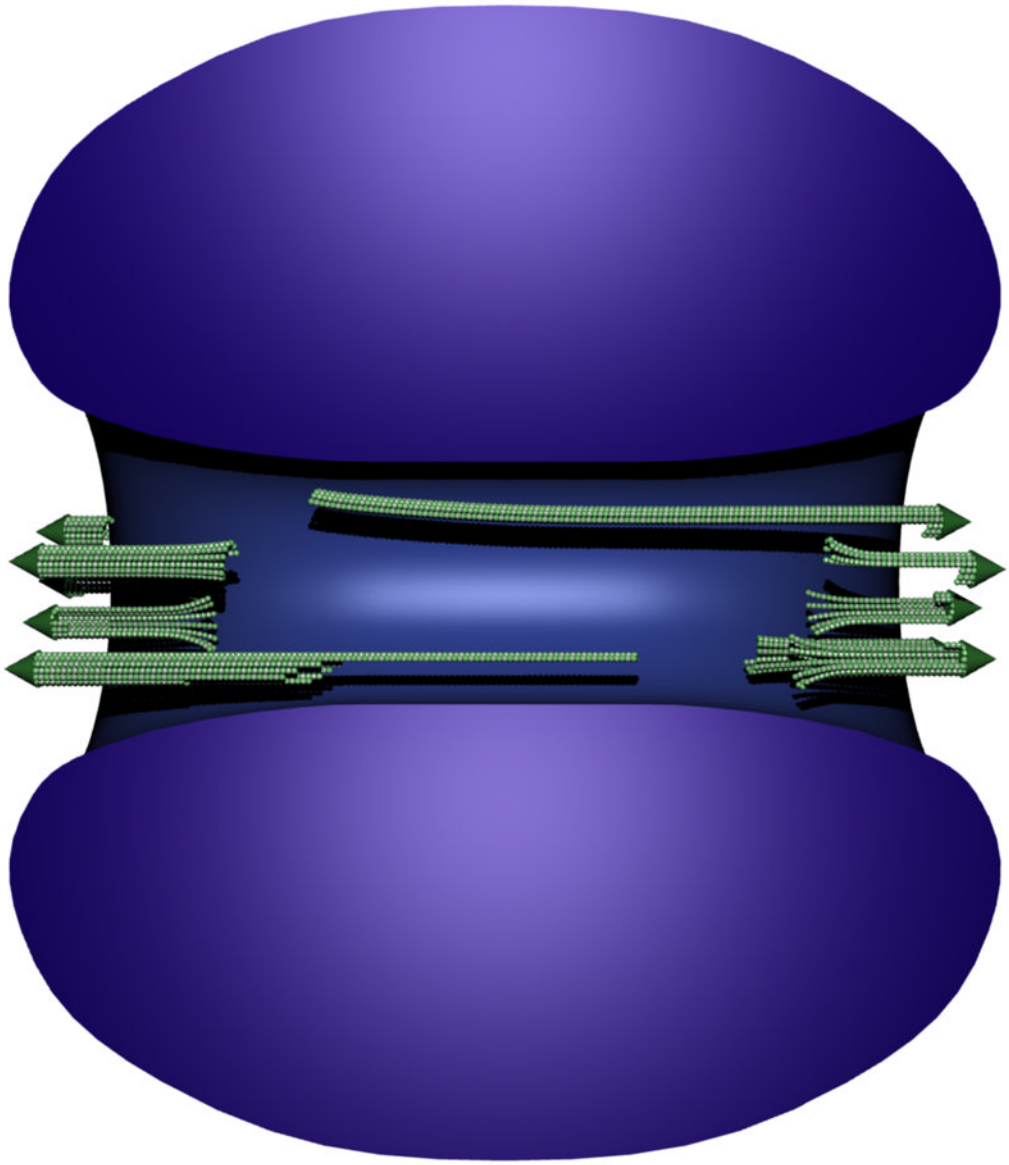

Figure 4. Organization of the *O. tauri* spindle

Scale model of the *O. tauri* spindle in the context of the chromatin. A small bundle of incomplete MTs (green) reside at each pole, and at most one long incomplete MT extends deep into the nucleus from each pole. Heterochromatin (blue) forms a torus-like structure with a central channel that we call the spindle tunnel. Individual chromosomes could not be resolved. The nuclear envelope (not shown) has openings at both spindle poles.